

# Statistical mechanics and ocean circulation

Rick Salmon

*Scripps Institution of Oceanography*

*UCSD 0213, 9500 Gilman Dr., La Jolla, CA 92093-0213 USA, email: rsalmon@ucsd.edu*

*Commun Nonlinear Sci Numer Simulat 17, 2144-2152 (2012)*

*doi:10.1016/j.cnsns.2011.05.044*

---

## Abstract

We apply equilibrium statistical mechanics based upon the conservation of energy and potential enstrophy to the mass-density distribution within the ocean, using a Monte Carlo method that conserves the buoyancy of each fluid particle. The equilibrium state resembles the buoyancy structure actually observed.

*Key words:* statistical mechanics, ocean circulation, Monte Carlo method

---

## 1. Introduction

Equilibrium statistical mechanics applies to systems of coupled ordinary differential equations of the form

$$\frac{dy_i}{dt} = f_i(y_1, y_2, y_3, \dots, y_n), \quad i = 1, \dots, n \quad (1.1)$$

where  $t$  is the time, and  $n$ , the number of degrees of freedom, is finite. Every state of the system with evolution equation (1.1) corresponds to a point  $\mathbf{y} \equiv (y_1, y_2, y_3, \dots, y_n)$  in phase space. If

$$\sum_{i=1}^n \frac{\partial f_i}{\partial y_i} = 0 \quad (1.2)$$

then the motion in phase space is non-divergent. If motion governed by (1.1) satisfying (1.2) conserves the  $m$  quantities  $E_1(\mathbf{y}), E_2(\mathbf{y}), \dots, E_m(\mathbf{y})$ , then equilibrium statistical mechanics predicts that the probability distribution in phase space approaches the canonical distribution

$$P(\mathbf{y}) = \alpha_0 \exp(-\alpha_1 E_1 - \alpha_2 E_2 - \dots - \alpha_m E_m) \quad (1.3)$$

where the  $m + 1$  constants  $\alpha_i$  are determined by the normalization requirement

$$\iint \dots \int d\mathbf{y} P(\mathbf{y}) = 1 \quad (1.4)$$

and by the  $m$  requirements

$$\langle E_i \rangle \equiv \iint \dots \int d\mathbf{y} E_i(\mathbf{y}) P(\mathbf{y}) = E_i^0 \quad (1.5)$$

that the average value of each  $E_i$  equals its prescribed value  $E_i^0$ . The distribution (1.3) maximizes the entropy

$$S = - \iint \dots \int d\mathbf{y} P \ln P \quad (1.6)$$

subject to the constraints (1.4) and (1.5). The  $\alpha_i$  are the Lagrange multipliers corresponding to these constraints. One can also regard  $\alpha_1, \alpha_2, \dots, \alpha_m$  as ‘inverse temperatures.’ If the microcanonical distribution is desired instead of (1.3), then additional constraints limiting the variance of the  $E_i$  may be attached to the maximization of (1.6). In most cases, the canonical and microcanonical distributions yield virtually identical results.

The equations of fluid mechanics fit the form (1.1) with Liouville property (1.2) if the viscosity and external forcing are neglected, and if the system is artificially truncated to a finite number of degrees of freedom. Such a

truncation always occurs in the construction of numerical models, in which the  $y_i$  correspond to gridded values of fluid velocity, pressure, etc., or to the amplitudes of Fourier modes. Thus we may regard (1.3) as the probability distribution, at  $t = \infty$ , of the dependent variables in a numerical model in which all the forcing and dissipation terms have been turned off. This equilibrium state represents the target state towards which nonlinear self-interactions drive the system. Additional insight is sometimes gained by considering the sequence of equilibrium states that occur as the truncation limit—the number of gridpoints or modes—is increased without bound.

In this paper, we apply the methods of equilibrium statistical mechanics to a model of the mass-density distribution in the ocean. It is a pleasure to dedicate this paper to my friend and colleague, Philip J. Morrison.

## 2. Background

The equilibrium statistical mechanics of macroscopic fluid motions enjoys an extensive literature. The pioneering papers are [1, 2, 3]. Lee [1] considered the case of three-dimensional flow governed by the incompressible Euler equations, with energy the only recognized invariant. In this case, the theory predicts equipartition of energy among Fourier modes corresponding to a wavenumber energy spectrum  $\mathcal{E}(k) \propto k^2$ . As the truncation wavenumber  $k_{max} \rightarrow \infty$ , all of the energy flows to infinitely high wavenumber, in rather bland agreement with general ideas about the direction of energy flow in three-dimensional turbulence.

Onsager [2] and Kraichnan [3] considered the much more interesting equi-

librium statistical mechanics of two-dimensional Euler flow governed by

$$\frac{\partial q}{\partial t} + J(\psi, q) = 0 \quad (2.1)$$

where  $\psi$  is the streamfunction for the flow with velocity  $\mathbf{u} = (u, v) = (-\psi_y, \psi_x)$  and  $q = \nabla^2\psi$  is the vorticity. Here  $\nabla A \equiv (A_x, A_y)$  and  $J(A, B) \equiv A_x B_y - B_x A_y$ . Subscripts denote differentiation. In the case of continuously distributed vorticity [3], equilibrium statistical mechanics based upon the conservation of energy

$$E = \frac{1}{2} \iint d\mathbf{x} (\nabla\psi \cdot \nabla\psi) \quad (2.2)$$

and enstrophy

$$Z = \frac{1}{2} \iint d\mathbf{x} q^2 \quad (2.3)$$

predicts an energy spectrum of the form

$$\mathcal{E}(k) = \frac{k}{\alpha_E + \alpha_Z k^2}. \quad (2.4)$$

The prescribed average values  $\langle E \rangle$  and  $\langle Z \rangle$  uniquely determine the inverse temperatures  $\alpha_E$  and  $\alpha_Z$ . Let the two-dimensional flow be confined to a domain of size  $k_0^{-1}$  with a maximum (truncation) wavenumber  $k_{max}$ . If  $k_{max} \rightarrow \infty$ , with  $k_0$ ,  $\langle E \rangle$  and  $\langle Z \rangle$  all held fixed, then all of the energy condenses onto the mode at  $k_0$ , and all of the ‘excess’ enstrophy  $\langle Z \rangle - k_0^2 \langle E \rangle$  moves toward infinite wavenumbers [4]. Thus the additional physical content of (2.3) renders the statistical mechanics of two-dimensional flow much more interesting and informative than the corresponding theory in three space dimensions. This trend continues as we consider quasi-geostrophic generalizations of (2.1), in which  $q$  acquires greater physical content.

The quasigeostrophic equations govern meso-scale motions in the atmosphere and ocean. Density stratification and the Earth’s rotation constrain these motions to be *quasi*-two-dimensional, hence the various forms of the quasigeostrophic equations correspond to generalizations of (2.1). For example, the quasigeostrophic equation governing an ocean consisting of a single-layer of homogeneous fluid is (2.1) with potential vorticity

$$q = \nabla^2\psi + \beta y + f_0 d(x, y)/H - f_0^2/gH \psi. \quad (2.5)$$

Here,  $(x, y)$  is the distance in the (east, north) direction with  $y = 0$  at the equator; the Coriolis parameter  $f = \beta y$  is twice the vertical component of the Earth’s rotation vector;  $f_0$  is a representative value of  $f$ ;  $d(x, y)$  is the ocean bottom elevation;  $g$  is the gravity constant; and  $H$  is the mean fluid depth. The last term in (2.5) represents the departure of the ocean surface elevation from its state of rest. The equilibrium statistical mechanics of (2.1,2.5) and its generalization to multi-layered flows were considered by [5]; for reviews, see [6, 7, 8]. The theory predicts a number of interesting features, including: the appearance of rectified mean flows  $\langle \psi(x, y) \rangle$  which arise from terms like the second and third terms on the rhs of (2.5); the depth-independence of the horizontal velocity on horizontal scales larger than the internal deformation radius; and the migration of kinetic energy toward the equator and into high vertical mode. As an example of relevance to the present paper, we consider single-layer quasigeostrophic flow governed by (2.1) and

$$q = \nabla^2\psi + \beta y \quad (2.6)$$

in which—compared to (2.5)—ocean bottom topography is neglected, and the ocean surface is replaced by a rigid lid.

The equilibrium statistical mechanics of (2.1, 2.6) in a bounded ocean, based on the conservation of energy (2.2), potential enstrophy (2.3), and circulation

$$C = \frac{1}{2} \iint d\mathbf{x} \ q \quad (2.7)$$

is thoroughly discussed in [9]. For simplicity, we here consider a square ocean, with the equator at mid-basin, in which the statistics are symmetrical about the equator. Then (2.7) vanishes by symmetry. In this case, the theory predicts a mean flow satisfying

$$\nabla^2 \langle \psi \rangle + \beta y = \frac{\alpha_E}{\alpha_Z} \langle \psi \rangle \quad (2.8)$$

and the boundary condition  $\langle \psi \rangle = 0$ , and a fluctuating flow  $\psi' = \psi - \langle \psi \rangle$  with the same spectrum (2.4) as in the  $\beta = 0$  case of plain, two-dimensional Euler flow. In this case, the limit  $k_{max} \rightarrow \infty$  of perfect model resolution produces a somewhat surprising result: Unless the energy is unrealistically large, the mean flow defined by (2.8) absorbs *all* of the energy, and all of the enstrophy in the fluctuating flow appears at infinite wavenumbers. That is, as  $k_{max} \rightarrow \infty$ , the flow approaches the quasi-steady state defined by (2.8), with all the fluctuations confined to infinitesimal lengthscales. For realistically small energy, the solution of (2.8) consists of a uniform westward interior flow with speed  $U_I \equiv \beta \alpha_Z / \alpha_E$  closed by boundary layers of width  $\sqrt{U_I / \beta} = \sqrt{\alpha_Z / \alpha_E}$ , as shown in Figure 1. Simple physical arguments based upon the conservation of potential vorticity (2.6) on fluid particles anticipate the appearance of such a westward mean flow, but the statistical-mechanics calculation is needed to confirm its true importance: In the asymptotic limit, the mean flow absorbs *all* of the energy in the system. This prediction has been confirmed by numerous numerical experiments [10, 11, 12].

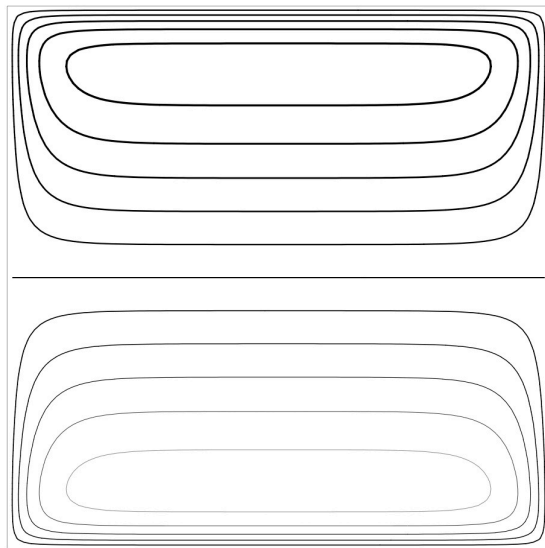


Figure 1: The solution  $\psi(x, y)$  of (2.8) in a square ocean. Larger values correspond to darker contours. The solution corresponds to a uniform, westward interior flow closed by inertial boundary layers. The parameters have been chosen to make the thickness of the inertial boundary layers equal to 5% of the ocean width.

The foregoing results invite a comparison between the predictions of equilibrium statistical mechanics and the time-average flow actually observed in the ocean. Unfortunately, such comparison must fail because quasigeostrophic dynamics is artificially constrained to situations in which the thickness of each fluid layer varies by only a small amount. For example, in the context of (2.5), we require  $|d|/H \ll 1$  and  $f_0|\psi|/gH \ll 1$ . In the context of continuously stratified quasigeostrophic theory, isopycnal surfaces cannot depart significantly from their position in a state of rest. However, as shown in Figure 2, observed isopycnal surfaces generally outcrop at the ocean surface. In models consisting of uniform-density layers, this outcropping corresponds to vanishing layer depth.

To overcome the inability of quasigeostrophic dynamics to accommodate vanishing layer depth, [13] considered the equilibrium statistical mechanics of a single fluid layer of depth  $h$  governed by shallow-water dynamics. This layer was regarded as the upper, moving layer of a two-layer ocean, in which the lower layer is infinitely deep and at rest. In the case of shallow-water dynamics, both the energy and the potential enstrophy

$$Z = \iint d\mathbf{x} \frac{(v_x - u_y + f)^2}{h} \quad (2.9)$$

are non-quadratic, hence it is impossible to calculate the equilibrium state analytically. Instead, [13] used a Monte Carlo method of calculation, in which, roughly speaking, fluid configurations are selected at random, and then accepted or rejected based upon their probability of occurrence in the canonical ensemble. Unfortunately, this random selection of fluid states confronts a severe technical challenge when the potential enstrophy takes the form (2.9): Vanishing of the layer depth  $h$  in (2.9) requires that the numer-

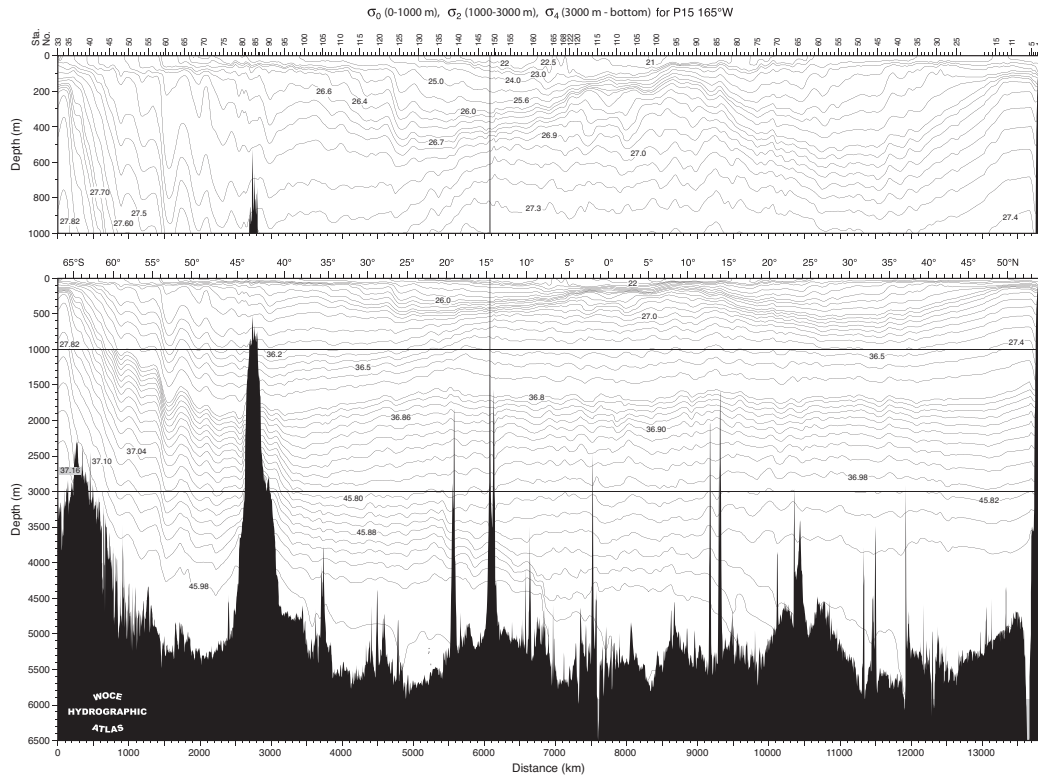


Figure 2: Potential density in a north/south section through the Pacific Ocean, at about the longitude of Hawaii. This figure may be compared to the theoretical sections of  $\langle \theta(y, z) \rangle$  shown in Figure 4. One unit of  $\sigma$  corresponds to about  $10^3$  units of  $\theta$  as defined in this paper. From the WOCE Pacific Ocean Atlas [16].

ator in (2.9) vanish simultaneously, and, in the Monte Carlo method, this must occur by chance. Although the mean state calculated by this method did in fact resemble Figure 2, the calculations in [13] proved to be extremely inefficient and contaminated by noise.

### 3. Continuously stratified formulation

In this paper, we reconsider the problem of calculating the statistical-mechanical mean state by a method that eschews quasigeostrophic dynamics yet avoids the technical difficulties of handling quotients like the one in (2.9). We begin by writing down the Boussinesq equations

$$\frac{D\mathbf{v}}{Dt} + f\mathbf{k} \times \mathbf{v} = -\nabla\phi + g\theta\mathbf{k} \quad (3.1a)$$

$$\nabla \cdot \mathbf{v} = 0 \quad (3.1b)$$

$$\frac{D\theta}{Dt} = 0 \quad (3.1c)$$

governing a three-dimensional, continuously stratified fluid. Here  $\mathbf{v} = (u, v, w)$ ,  $D/Dt \equiv \partial/\partial t + \mathbf{v} \cdot \nabla$ , and  $\mathbf{k}$  is the vertical unit vector.  $\phi$  is the pressure divided by a constant representative value  $\rho_0$  of the mass density  $\rho$ . The buoyancy is defined as  $\theta \equiv -\delta(\rho - \rho_0)/\rho_0$ . The ‘dynamical cores’ of ocean general circulation models are based upon equations very similar to (3.1). These models typically use ocean temperature and salinity instead of buoyancy  $\theta$ , but in the presently considered case of ideal, inviscid, non-diffusive flow, this difference is irrelevant.

From the viewpoint of equilibrium statistical mechanics, only the forms of the conserved quantities have any bearing on the results. The dynamics

(3.1) conserves energy in the form

$$E = \iiint d\mathbf{x} \left( \frac{1}{2} \mathbf{v} \cdot \mathbf{v} - gz\theta \right) \quad (3.2)$$

and every quantity of the form

$$\iiint d\mathbf{x} F(\theta, q) \quad (3.3)$$

where  $F$  is an arbitrary function, and

$$q = (\nabla \times \mathbf{v} + f\mathbf{k}) \cdot \nabla\theta \quad (3.4)$$

is the potential vorticity. The form of (3.3) reflects the fact that both buoyancy and potential vorticity are conserved on fluid particles,  $D\theta/Dt = Dq/Dt = 0$ , and that the fluid is incompressible. Potential enstrophy corresponds to the choice  $F(\theta, q) = q^2$ .

One can apply the machinery of equilibrium statistical mechanics directly to (3.2) and some choices of (3.3). However, preliminary calculations suggest that the results are unphysical and therefore uninteresting. For example, one finds that the average velocity  $\langle \mathbf{v} \rangle$  freely crosses surfaces of constant  $\langle \theta \rangle$ . This occurs because absolutely nothing in the form of the invariants (3.2-3) prevents it. Evidently, equilibrium statistical mechanics is valuable only if the conservation laws constrain the physics sufficiently, that is, only if leading-order dynamical balances are built into the forms of the energy and potential enstrophy. Quasigeostrophic dynamics builds in the fundamental geostrophic and hydrostatic balances. In contrast, there is no imposed relationship between the velocity  $\mathbf{v}$  and the buoyancy  $\theta$  in (3.2-4).

Planetary geostrophic dynamics, which is simpler even than quasigeostrophic dynamics but not subject to the latter's artificial restriction to nearly uni-

form layer depths, is obtained by dropping the term  $D\mathbf{v}/Dt$  in (3.1a). The resulting equations conserve energy in the form

$$E = \iiint d\mathbf{x} (-gz\theta) \quad (3.5)$$

and (3.3) with potential vorticity

$$q = \beta y \theta_z. \quad (3.6)$$

These are the ‘hydrographer’s’ forms of energy and potential vorticity, in which the kinetic energy and relative vorticity  $\nabla \times \mathbf{v}$  are neglected. Such neglect is justified by the facts that most of the energy associated with the large-scale ocean flow is potential energy, and the large-scale relative vorticity is almost everywhere much smaller than the planetary vorticity  $f$ . That is, the Rossby number is small.

In this paper we compute  $\langle \theta \rangle$ , the average of all buoyancy fields  $\theta$  with specified values of the energy (3.5) and

$$\iiint d\mathbf{x} F(\theta, \beta y \theta_z) \quad (3.7)$$

for some choices of the arbitrary function  $F$ . Particular importance attaches to conserved quantities of the form

$$\iiint d\mathbf{x} F(\theta) \quad (3.8)$$

because conservation of (3.8) for arbitrary  $F$  implies the conservation of volume within every range of buoyancy. Thus (3.8) *defines* the system under consideration, and we therefore demand that it be exactly conserved, for any function  $F$ . To achieve this, we adopt Monte Carlo perturbations that

consist of interchanges of pairs of fluid particles, in a manner explained more fully below. The general conserved quantity (3.7) includes potential-vorticity moments of the form

$$Z_n[F] \equiv \iiint d\mathbf{x} F(\theta)(\beta y \theta_z)^n. \quad (3.9)$$

By cross-equatorial symmetry,  $Z_n$  vanishes for all odd  $n$ . Thus  $Z_2$  is the lowest order non-vanishing moment, and it is the moment usually considered to be the most important in determining the statistical mechanical equilibrium state. If  $F \equiv 1$  then

$$Z \equiv Z_2[1] = \iiint d\mathbf{x} (\beta y \theta_z)^2 \quad (3.10)$$

is the total potential enstrophy of the system. If, on the other hand,  $F = \delta(\theta - \theta_0)$ , then  $Z_2[F]$  is the potential enstrophy on the constant-buoyancy surface  $\theta = \theta_0$ . In this paper we consider the total potential enstrophy (3.10) as the only potential enstrophy invariant. Thus our calculations correspond to averages over all the system states with given values of energy (3.5) and total potential enstrophy (3.10), where the number of fluid particles with any given value of buoyancy is the same in every state.

Our choice of (3.10) over the many possibilities allowed by (3.9) follows the many previous workers who regard energy and potential enstrophy as the dynamical invariants of greatest importance. As justification for this, we subscribe to the argument given in [9] that ‘...the complicated interleaved hypersurfaces [corresponding to the higher,  $n > 2$ , moments of vorticity] intersect the energy-enstrophy hypersurface in a way which samples *that* surface well, and so coarse-grained averages are accurately obtained simply by averages over the intersection of the energy and enstrophy hypersurfaces.’ See

[13] for further discussion, and for a calculation in which the *fourth* moment of the potential enstrophy was included in a Monte Carlo calculation. By basing the calculations of the present paper on the energy (3.5) and the total potential enstrophy (3.10) we keep the number of adjustable parameters to a minimum; every additional invariant of the form (3.9) would introduce an additional temperature. It seemed more impressive to obtain realistic results with the smallest number of adjustable parameters.

The conserved quantities (3.5) and (3.10) contain  $y$  and  $z$ —but not  $x$ —as parameters. We therefore anticipate that the equilibrium statistics are independent of  $x$ , to the extent allowed by the no-normal-flow boundary conditions. For simplicity, we consider a rectangular ocean, centered on the equator, with a flat bottom, rigid lid, and vertical sidewalls. Boundary currents at the eastern and western boundaries must exist to close the interior flow, but throughout the ocean interior the average flow is  $x$ -independent, like the solution of (2.8) shown in Figure 1. In this paper, we calculate only this  $x$ -independent part of the flow. The state of the system then corresponds to the single two-dimensional field  $\theta(y, z)$ , which we represent by the gridded values  $\theta_{jk} = \theta(j\Delta y, k\Delta z)$ , where  $\Delta y$  and  $\Delta z$  are grid spacings in the northward and vertical directions, respectively. No boundary conditions on  $\theta(y, z)$  are required; although  $\partial\theta/\partial y$  determines the vertical derivative  $\partial u/\partial z$  of the eastward geostrophic velocity  $u$ , this component of the velocity is directed ‘into the page’. Let  $n_y$  and  $n_z$  be the number of grid points in the northward and vertical directions. Then the dimension of our phase space is  $n = n_y n_z$ .

To calculate ensemble averages at equilibrium, we use a Monte Carlo method based upon the Metropolis algorithm [14]. To begin the algorithm,

we assign the buoyancy values  $\theta_{jk} = \theta_{ref}(k\Delta z)$  corresponding to the horizontally uniform, reference state

$$\theta_{ref}(z) = \theta_0 e^{z/d}. \quad (3.11)$$

Here,  $\theta_0$  is the uniform reference buoyancy at the ocean surface  $z = 0$ , and  $d$  is a constant. The reference state (3.11) serves only to fix the *distribution* of buoyancy values on fluid particles. The Monte Carlo algorithm consists of a series of sweeps through all the grid points in our system. At each gridpoint  $(j, k)$  we select another grid point  $(j', k')$  at random, and we nominate the system state corresponding to an interchange of buoyancy values between these two grid points as the next state in our ensemble. If, according to the canonical probability distribution,

$$P = \alpha_0 \exp(-\alpha_E E - \alpha_Z Z), \quad (3.12)$$

this state is *more* probable than the former state, then we accept the new state as the next state of our ensemble. If, on the other hand, the new state is *less* probable than the previous state according to (3.12), then we accept it with probability equal to the ratio of the probabilities of the two states. It can be shown (e.g. [15], pp 64-72) that this process of accumulating ensemble members eventually results in an ensemble of states in which each state occurs with the same probability as in the canonical distribution. To compute the average  $\langle G \rangle$  of any quantity  $G[\theta(y, z)]$  that depends on the system state, we simply add up all the values of  $G$  in our accumulated ensemble and divide by the number of ensemble members. Each ensemble member is a rearrangement of the beginning, reference state (3.11) and therefore contains the same number of gridpoints with any given value of buoyancy. Thus we

treat all the Casimirs of the form (3.8) as in the microcanonical ensemble; all these invariants are ‘statistically sharp.’ However, we must choose values for  $\alpha_E$  and  $\alpha_Z$ . These uniquely determine the *average* values,  $\langle E \rangle$  and  $\langle Z \rangle$ , of the canonical invariants (3.5) and (3.10). The normalization constant  $\alpha_0$  in (3.12) is irrelevant, because the algorithm depends only on the ratio of probabilities.

#### 4. Results

We consider a rectangular ocean of depth  $H = 3\text{km}$ , extending a distance  $L = 4000\text{km}$  to either side of the equator. With  $n_y = 200$  and  $n_z = 100$ , the grid spacings are  $\Delta y = 40\text{km}$  and  $\Delta z = 30\text{m}$ . For the reference state, we take (3.11) with  $\theta_0 = 0.002$  and  $d = 1\text{km}$ . Since the Monte Carlo perturbations consist of pairwise buoyancy exchanges between gridpoints, the area corresponding to any range of buoyancy will always be the same as in this reference state. Henceforth we regard the  $E$  and  $Z$  in (3.12) as the *volume averages* of the energy (3.5) and potential enstrophy (3.10). That is, we normalize the conserved quantities by dividing by the number of grid points.

First we consider the case  $\alpha_Z = 0$  in which potentially enstrophy is wholly unconstrained. The equilibrium state  $\langle \theta \rangle$  then depends solely on  $z$  and on the parameter  $\alpha_E$  in (3.12). Figure 3 shows  $\langle \theta(z) \rangle$  for several values of the ‘energy temperature’  $T_E \equiv 1/\alpha_E$ . At low temperatures, the equilibrium buoyancy profile is very close to its ‘ground state’ (3.11), which is shown as curve a. As the energy temperature increases (curves b-f), the equilibrium profile becomes more uniform. At very high  $T_E$ , the gravity force is insignificant; each buoyancy value occurs with equal probability at all vertical levels, and

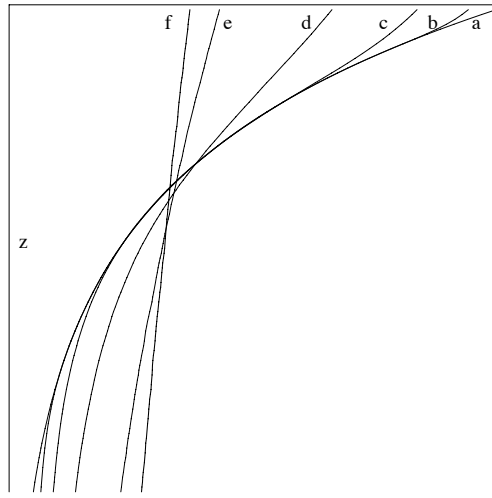


Figure 3: Vertical profiles of the average buoyancy  $\langle \theta(z) \rangle$  at various values of the energy temperature  $T_E = \alpha_E^{-1}$ . The corresponding values of vertical fluid particle displacement  $\delta$  are: (a) 0, (b) 0.1, (c) 0.3, (d) 0.5, (e) 1.0, and (f) 1.5 km. Curve (a) corresponds to the reference state of rest defined by (3.11). The upper, horizontal line corresponds to the ocean surface. The ocean depth is 3 km.

the equilibrium buoyancy is independent of  $z$  at a value equal to the  $z$ -average of (3.11). Individual ensemble members may contain regions of static instability, but the equilibrium buoyancy always obeys  $\partial\langle\theta\rangle/\partial z > 0$ .

The physically interesting regime is the one in which  $T_E$  is large enough to allow significant departures from (3.11) but not so large as to render buoyancy forces insignificant. To estimate this value, let us first agree to measure energy relative to the ground state. This amounts to regarding  $E$  as the available potential energy  $A$ . As a rough estimate of available potential energy (per unit volume) we take

$$A \sim g \frac{d\theta_r}{dz} \delta^2 \sim \frac{g\theta_0\delta^2}{d} \quad (4.1)$$

where  $\delta$  is the average vertical displacement of fluid particles from their position in the reference state. Then

$$T_E = \frac{g\theta_0\delta^2}{nd}, \quad (4.2)$$

where  $n = n_y n_z$  is the number of grid points, provides a convenient definition of the energy temperature in terms of the estimated particle displacement. All of the buoyancy profiles in Figure 3 are labeled with  $\delta$  defined by (4.2) rather than by  $T_E$ . Judging by Figure 3, these values of  $\delta$  provide reasonable estimates of the mean vertical fluid-particle displacement. For example, curve c in Figure 3 corresponds to a value of  $T_E$  for which (4.2) gives  $\delta = 0.3$  km. Recalling that the ocean depth in Figure 3 is 3 km, we see that curve c does indeed depart from curve a ( $T_E = 0$ ) at a depth of about 0.3 km. In all subsequent calculations, we use this value of  $T_E$ .

Next we consider equilibrium states in which both the energy and the potential enstrophy are constrained. For the potential enstrophy temperature

$T_Z \equiv 1/\alpha_Z$  we take

$$T_Z = s \frac{f_{max}^2 \theta_0^2}{d^2 n} \quad (4.3)$$

where  $s$  is a non-dimensional parameter, and  $f_{max}$  is the value of the Coriolis parameter at the northern boundary of the ocean. Once again, Figure 3 corresponds to infinite potential enstrophy temperature,  $s = \infty$ . The potential enstrophy constraint becomes significant as  $s$  decreases from infinity to the order-one values that characterize the observed ocean. Figure 4 shows the average buoyancy  $\langle \theta(y, z) \rangle$  in four north/south sections corresponding to 4 values of the potential enstrophy temperature (4.3). Figure 4 may be compared to the observed buoyancy shown in Figure 2. The resemblance between observations and theory is greatest for intermediate values of potential enstrophy temperature, corresponding to  $s = 10$  (Figure 4b) and  $s = 1$  (Figure 4c), as anticipated by our scaling analysis. By the ‘thermal wind’ relation, isopycnals that slope upward away from the equator correspond to positive values of  $\partial u / \partial z$  (and conversely), where  $u$  is the eastward geostrophic velocity. Thus the equatorial ‘lump’ in buoyancy that appears in Figures 2 and 4 corresponds to relatively strong eastward current at mid-depth. This Equatorial Undercurrent is a prominent feature of the observed ocean circulation. Its appearance in a calculation based upon equilibrium statistical mechanics was wholly unanticipated. Prevailing theories of the Undercurrent are strongly based upon the pattern of winds in the equatorial ocean. Figure 4 shows that the width of the equatorial undercurrent does not scale as the equatorial deformation radius. Instead it is amplitude dependent; the Undercurrent narrows as the potential enstrophy temperature  $T_Z$  decreases.

Most oceanographers would maintain that the double-lobe shape of upper-

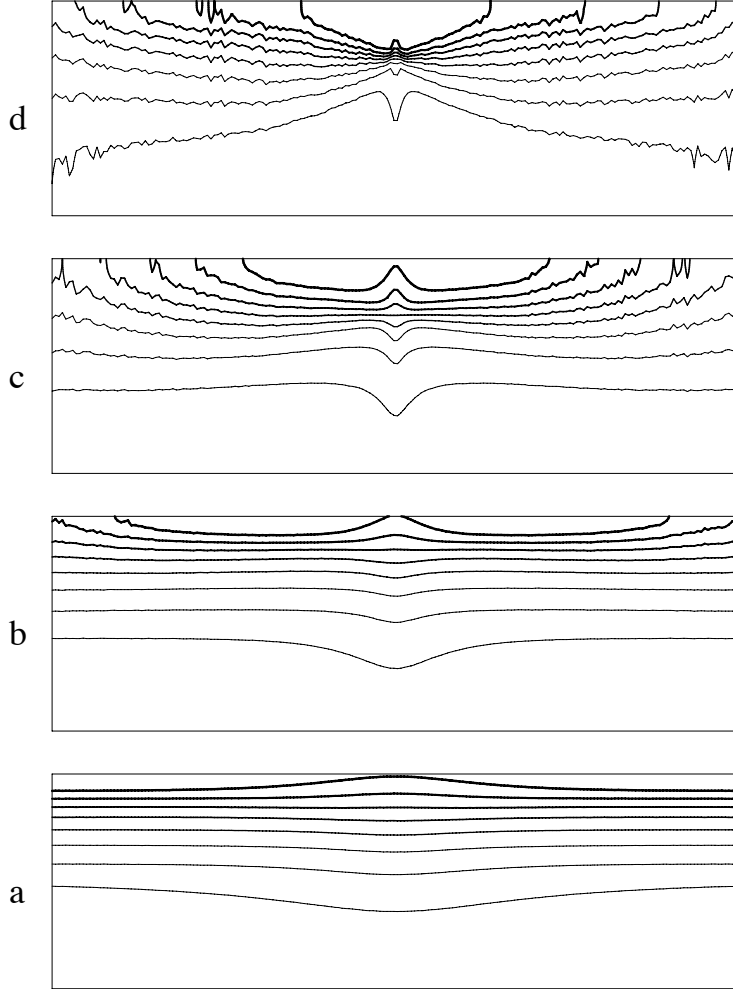


Figure 4: North-south sections of average buoyancy  $\langle \theta(y, z) \rangle$  at various values of the potential enstrophy temperature  $T_Z = \alpha_Z^{-1}$ . The energy temperature, corresponding to  $\delta = 0.3\text{km}$  in (4.2), is the same in all cases. The potential enstrophy temperatures correspond to (a)  $s = 100$ , (b)  $s = 10$ , (c)  $s = 1$ , and (d)  $s = 0.1$  in (4.3). Each section is 8000 km wide by 3 km deep, with the equator at the middle. Darker lines correspond to larger values of the buoyancy.

ocean isopycnals common to Figures 2 and Figure 4 is the result of a particular wind forcing, and that the decrease in ocean surface buoyancy with latitude has at least something to do with the fact that solar heating is greatest at the equator. However, Figure 4 is simply the average over all the system states with given values of energy and potential enstrophy; it represents the average that would be observed if the rest state (3.11) were subjected to a temporary, random, adiabatic stirring, and if an infinite amount of time were allowed to elapse after the stirring had ceased. In a sense, equilibrium statistical mechanics does not actually *explain* any of the realistic features in Figure 4. Rather, it suggests that these features require no particular explanation at all.

### **Acknowledgment**

Work supported by the National Science Foundation, OCE-0542890. I thank Lynne Talley and Sharon Escher for their help with Figure 2.

### **References**

- [1] Lee TD. On some statistical properties of hydrodynamical and magneto-hydrodynamical fields. Q J Appl Math 1952; 10: 69-74.
- [2] Onsager L. Statistical hydrodynamics. Nuovo Cimento 1949; 6, Suppl: 279-287.
- [3] Kraichnan RH. Inertial ranges in two-dimensional turbulence. Phys Fluids 1967; 10: 1417-1423.
- [4] Kraichnan RH. Statistical mechanics of two-dimensional flow. J Fluid Mech 1975; 67: 155-175.

- [5] Salmon R, Holloway G, Hendershott MC. The equilibrium statistical mechanics of simple quasi-geostrophic models. *J Fluid Mech* 1976; 75: 691-703.
- [6] Salmon R. Geostrophic turbulence *in* *Topics in Ocean Physics*, Corso LXXX Enrico Fermi School, AR Osborne and PM Rizzoli eds. Amsterdam: North Holland; 1982.
- [7] Holloway G. Eddies, waves, circulation and mixing: Statistical geofluid mechanics. *Ann Rev Fluid Mech* 1986; 18: 91-147.
- [8] Salmon, R. *Lectures on Geophysical Fluid Dynamics*. New York: Oxford; 1998.
- [9] Carnevale G, Frederiksen JD. Nonlinear stability and statistical mechanics of flow over topography. *J Fluid Mech* 1987; 175: 157-181.
- [10] Griffa A, Salmon R. Wind-driven ocean circulation and equilibrium statistical mechanics. *J Mar Res* 1989; 47: 457-492.
- [11] Dukowicz JK, Greatbatch RJ. Evolution of mean-flow Fofonoff gyres in barotropic quasigeostrophic turbulence. *J Phys Oc* 1999; 29: 1832-1852.
- [12] Wang J, Vallis GK. Emergence of Fofonoff states in inviscid and viscous ocean circulation. *J Mar Res* 1994; 52: 83-127.
- [13] Salmon R. The shape of the main thermocline, revisited. *J Mar Res* 2010; in press.

- [14] Metropolis N, Rosenbluth A, Rosenbluth MN, Teller AH, Teller E. Equation of state calculations by fast computing machines. *J Chem Phys* 1953; 21: 1087-1092.
- [15] Kalos MH, Whitlock PA. *Monte Carlo Methods*, 2d ed. Weinheim: Wiley-VCH; 2008.
- [16] Talley LD. *Hydrographic Atlas of the World Ocean Circulation Experiment (WOCE). Volume 2: Pacific Ocean* (eds. M. Sparrow, P. Chapman and J. Gould), International WOCE Project Office, Southampton, UK, ISBN 0-904175-54-5; 2007.